OMTN, Volume *34*

Supplemental information

Targeting lung cancer with clinically relevant EGFR mutations using anti-EGFR RNA aptamer

Brian J. Thomas, Caitlyn Guldenpfennig, Yue Guan, Calvin Winkler, Margaret Beecher, Michaela Beedy, Ashley F. Berendzen, Lixin Ma, Mark A. Daniels, Donald H. Burke, and David Porciani

SUPPLEMENTAL INFORMATION

Figure S1

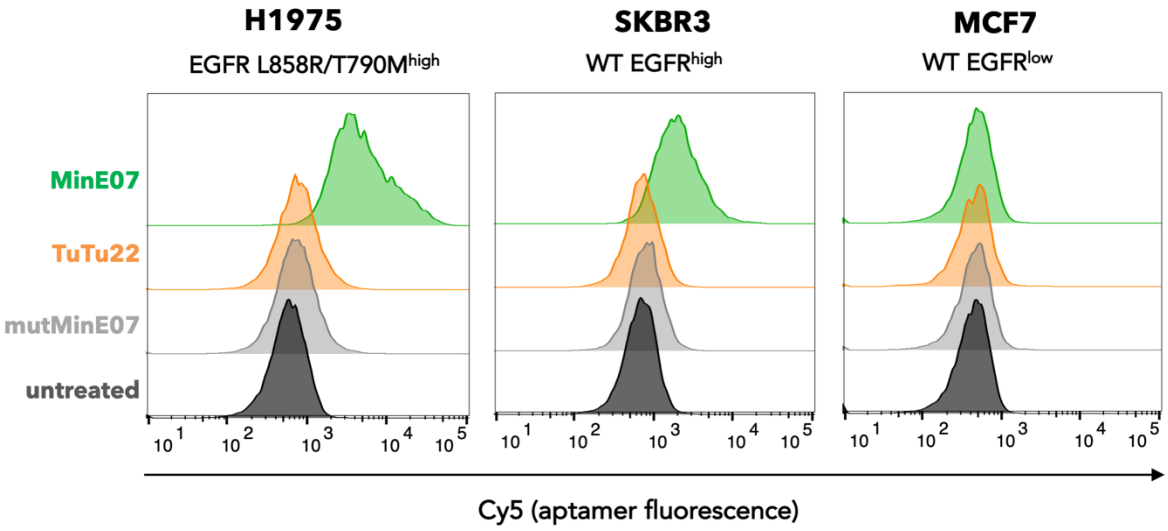

Figure S1. Cell labeling comparison between anti-EGFR RNA (MinE07) and DNA (TuTu22) aptamers. Prior to the incubation with the cells, all aptamers (MinE07, green; TuTu22, orange: mutMinE07, grey) bearing a 3-end tail sequence $(CGA)_7$ sequence were annealed to a Cy5-labeled DNA anti-tail (as described in the materials and methods section). Aptamers were then incubated for 1 hour at 37°C with H1975 (NSCLC cells) or two breast cancer cell lines, such as SKBR3 (high EGFR expression), and MCF7 (low EGFR expression). Flow cytometry assays were performed to define extent of cell labeling. Representative histograms from one of n=2 independent experiments are shown. MinE07 showed an increased cell staining of H1975 and SKBR3 cells that express high levels of EGFR (mutant L858R/T790M and wild type EGFR, respectively), while showing a reduced labeling of MCF7 cells (low EGFR). In contrast, TuTu22 did not effectively stain H1975 and SKBR3 cells as MinE07 did, but showed minimal background binding in all cell lines, similar to the control aptamer (mutMinE07). The TuTu22 aptamer sequence used is reported as follows (3'-tail is underlined):
TACCAGTGCGATGCTCAGTGCCGTTTCTTCTCTTTCGCTTTTTTTGCTTTTGAGCATGCTGACGCATT
CGGTTGAC<u>CGACGACGACGACGACGACGA.</u> Note that TuTu22 aptamer sequence was modified to include the 3'-tail which could have altered aptamer folding and subsequent binding properties during comparative studies.

Figure S2

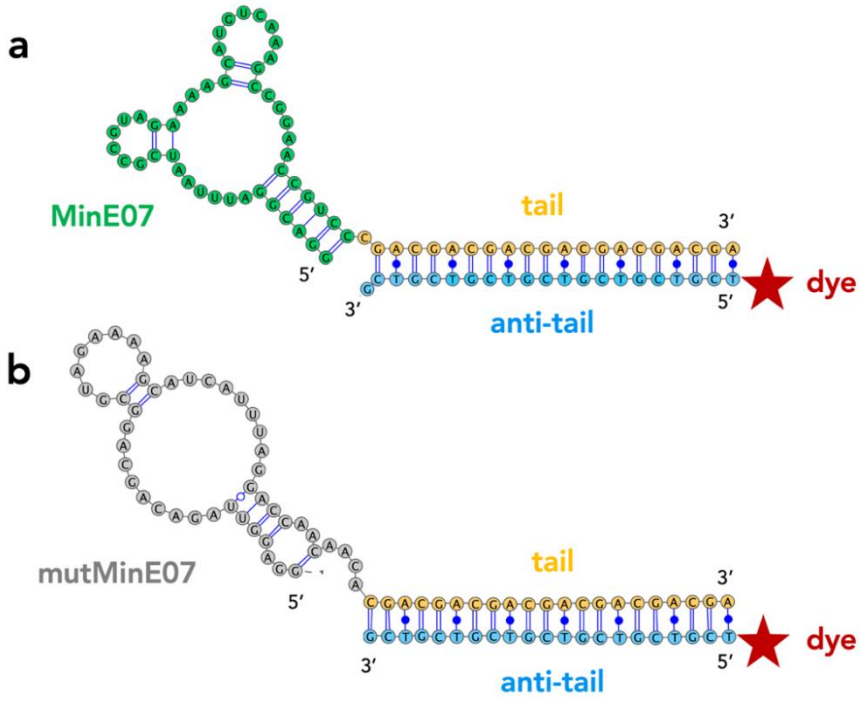

Figure S2. Schematic of labeling RNA aptamers using tail/anti-tail hybridization.
2'FY RNA aptamers (MinE07, green; mutMinE07, grey) were extended with a 21 nt tail sequence (yellow) at the 3' end. Aptamers were annealed/hybridized to a DNA anti-tail (blue) that was conjugated to a dye (red star) at the 5' end. Tail/anti-tail annealing/hybridization was also used to engineer bispecific aptamers.

Figure S3

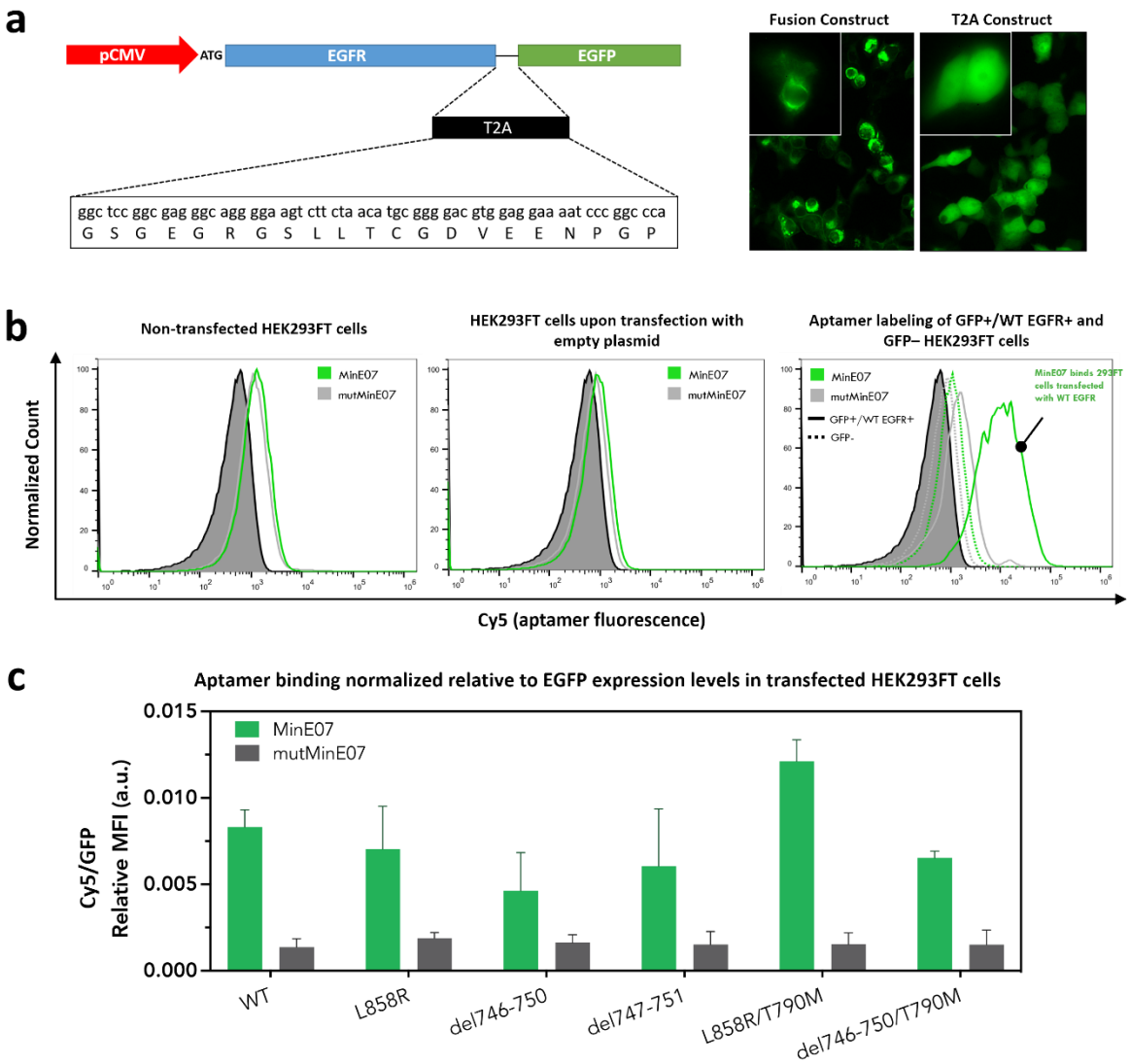

Figure S3. MinE07 aptamer binds cell-surface EGFRs transfected on HEK293FT cells and shows minimal background of non-transfected HEK293FT cells (GFP- cells).
(**a**) Map of relevant features from expression plasmid used to transfect HEK293FT cells. Representative images (20X, inset 100X) show GFP localization of fusion construct and upon introduction of the T2A segment. (**b**) Upon 45 min incubation with 100 nM Cy5-labeled anti-EGFR aptamer (MinE07, green) or negative control aptamer (mutMinE07, grey), flow cytometry histograms display minimal background labeling of HEK293FT cells that were either non-transfected (left, a) or transfected with an empty plasmid (middle, a). However, in the histograms on the right (a), MinE07 shows improved labeling of GFP+ HEK293FT cells transfected with WT EGFR, while maintaining minimal background binding of GFP- cells (*i.e.*, non-transfected HEK293FT cells within the same well). (**c**) Cy5-labeled MinE07 cell staining was normalized based on the GFP fluorescence levels in the transfected GFP+ HEK293FT cells. Relative MFIs (expressed as MFI_{Cy5}/MFI_{GFP}) confirmed that MinE07 retains its ability to target EGFR even when harboring mutations in the TKD. Plotted values represent mean ± SD for n=3 independent experiments.

Figure S4

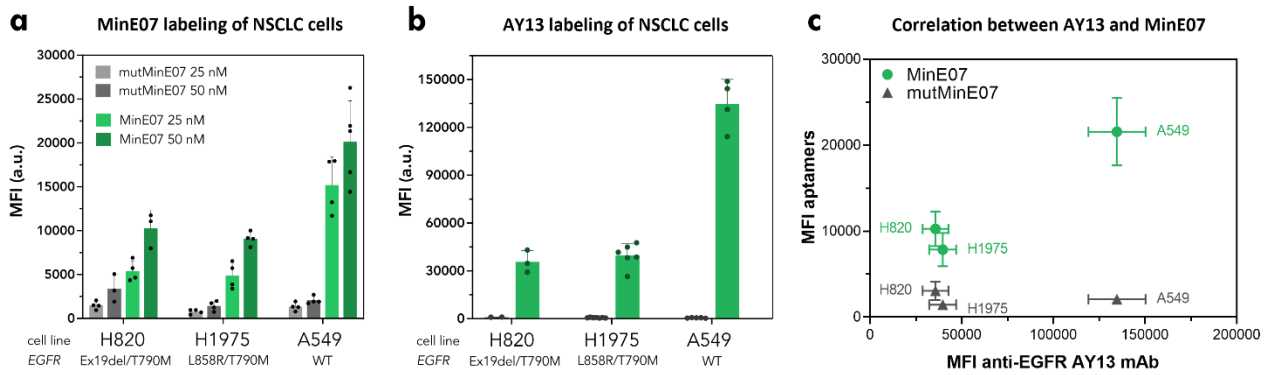

Figure S4. MinE07 aptamer and anti-EGFR antibody labeling of NSCLC cell lines expressing variable amounts of endogenous EGFR.
NSCLC cell lines expressing endogenous mutant (H820, H1975) or WT (A549) EGFR were incubated with (**a**) either 25 nM (light) or 50 nM (dark) Atto647N-labeled anti-EGFR aptamer (MinE07, green bar) or negative control aptamer (mutMinE07, grey) or (**b**) 4 nM of APC labeled anti-EGFR antibody (clone AY13, green bar) or isotype control (grey bar). Relative aptamer labeling is consistent with antibody staining and EGFR expression in the literature for these cell lines. Plotted values (a, b) represent mean ± SD for n=3-5 independent experiments. (**c**) Scatter plot analysis correlates average MFIs of anti-EGFR AY13 mAb (*x*-axis) with the average MFIs (at 50 nM) of MinE07 (green circle, *y*-axis) and mutMinE07 (grey triangle, *y*-axis). Pearson's correlation coefficient for MinE07 compared to the AY13 mAb is r = 0.9798 (P=0.1283), and R squared = 0.9600. In contrast, in the case of mutMinE07 r = -0.1570 (P= 0.8996), and R squared = 0.02465. Note, horizontal error bars refer to the standard deviation in the MFI values of AY13, while the vertical error bars correspond to the standard deviation of MFIs of MinE07 (green) or mutMinE07 (grey).

Figure S5

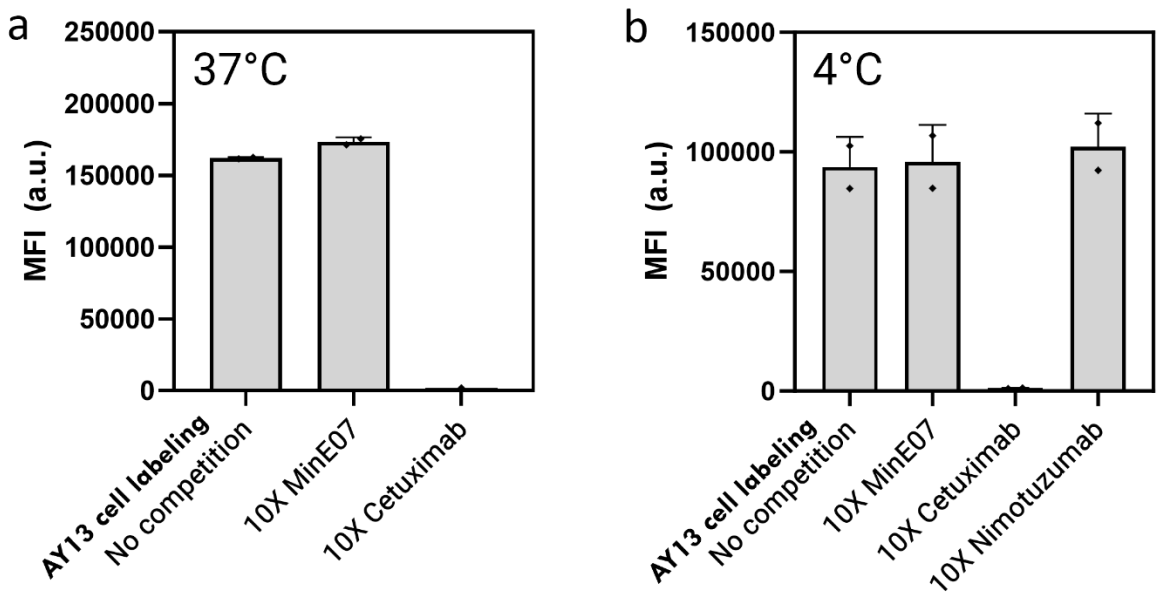

Figure S5. MinE07 aptamer does not compete with anti-EGFR antibody clone AY13.
H1975 cells (NSCLC cell line expressing endogenous EGFR L858R/T790M) were incubated with 50 nM APC labeled anti-EGFR antibody (clone AY13) and either PBS (no competition) or 10X competitors (500 nM) for 45 minutes at (**a**) 37°C, or at (**b**) 4°C to mitigate receptor internalization. Cells were then analyzed via flow cytometry. The data show that aptamer MinE07 and nimotuzumab do not compete with anti-EGFR antibody AY13 whereas cetuximab does compete. Plotted values represent mean ± SD for n=2 independent experiments

Figure S6

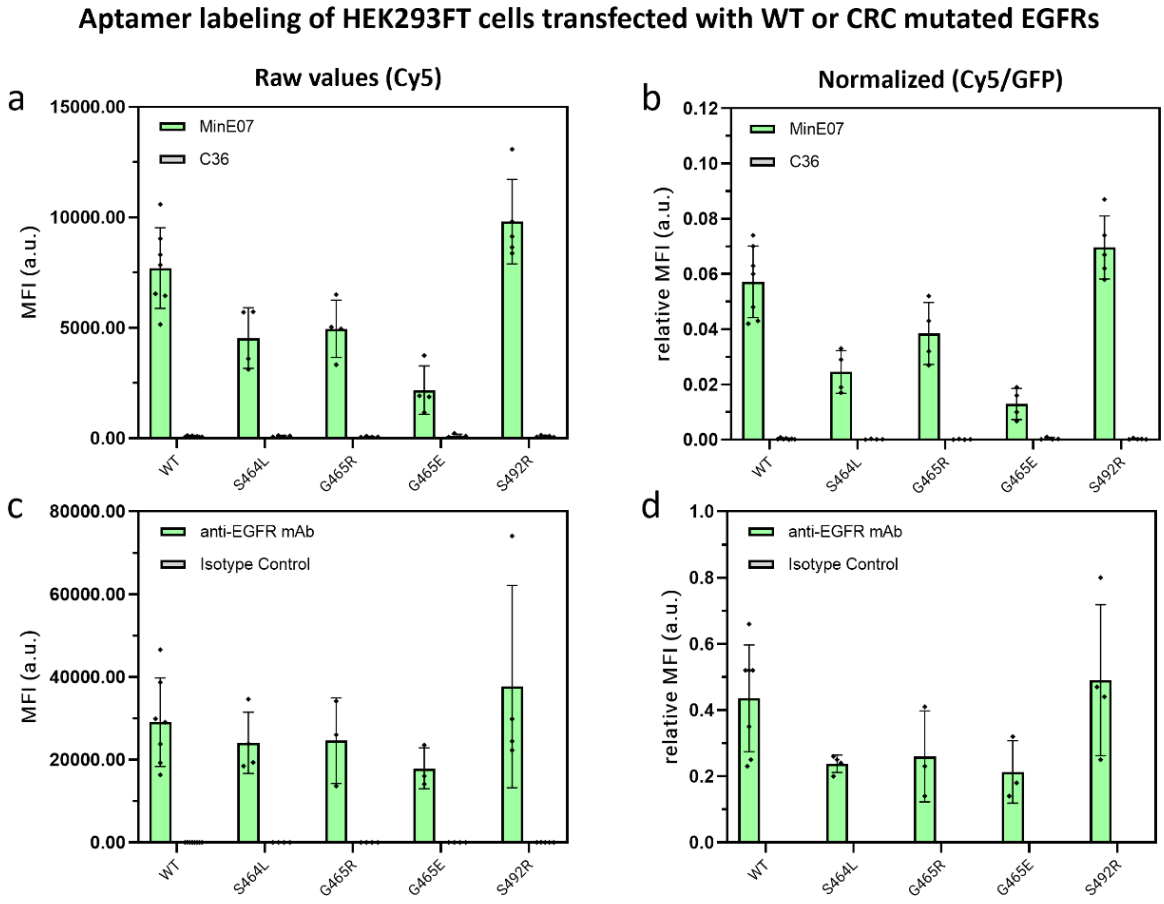

Figure S6. Anti-EGFR aptamer labeling of HEK293FT cells transfected with clinically relevant mutant EGFRs expressed in colorectal cancer in response to cetuximab treatment.
HEK293FT cells were transfected with an expression plasmid containing either WT or mutant EGFR (domain III) and an EGFP reporter under control of the pCMV reporter (pCMV_EGFR_T2A_EGFP, Table S1). Transfected cells were incubated with (**a, b**) 100 nM Cy5 labeled anti-EGFR aptamer (MinE07, green bar) or control aptamer (mutMinE07, grey bar) or (**c, d**) 1.3 ug/ml APC labeled anti-EGFR antibody (clone AY13, green bar) or isotype control (grey bar) for 45 min at 37°C and analyzed via flow cytometry. Cy5 mean fluorescence intensity (MFI; a, c) or normalized MFI (Cy5/GFP; b, d) of GFP+ cells is reported on the *y*-axis. Antibody labeling confirmed that introduced mutations did not significantly alter receptor trafficking to the cell surface compared to WT receptor. MinE07 labeling was decreased in cells expressing EGFR S464L, G465R, and G465E compared to WT but was not affected by the S492R mutation. Plotted values (a-d) represent mean ± SD for n=3-6 independent experiments.

Figure S7

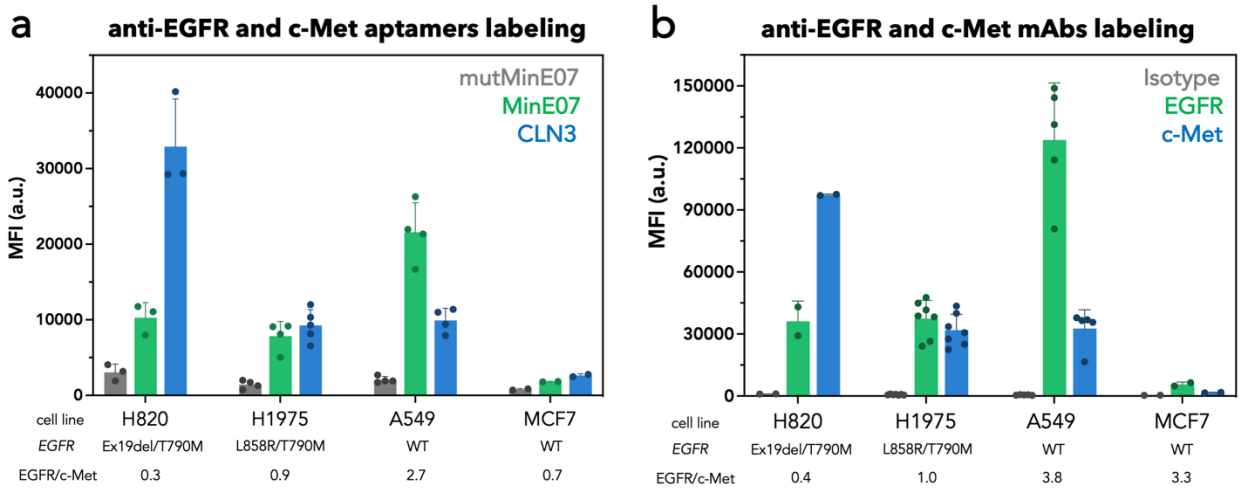

Figure S7. Relative cell labeling using anti-EGFR and anti-c-Met aptamers and mAbs
Cell lines harboring moderate to high levels (H820, H1975, A549) or very low levels (MCF7) of endogenous EGFR (WT or mutant) and c-Met (WT only) were incubated with (**a**) 50 nM Atto647N-labeled anti-EGFR (MinE07, green bar) or anti-c-Met (CLN3, blue bar) monospecific aptamer, or control aptamer (mutMinE07, grey bar) or with (**b**) 50nM APC-labeled anti-EGFR (clone AY13, green bar) or anti-c-Met (clone 271, blue bar) antibody, or isotype control (grey bar) for 1 hr at 37°C and analyzed via flow cytometry. For cell lines expressing moderate to high levels of antigens, relative EGFR/cMet aptamer labeling is consistent with antibody staining and EGFR/c-Met expression profiles in the literature for these cell lines. For MCF7, which express none or very low levels of antigens, relative labeling is inconsistent. This is likely due to differences in non-specific binding properties between the two probing agents when antigen expression is very low. Plotted values (a, b) represent mean ± SD for n=2-7 independent experiments

Figure S8

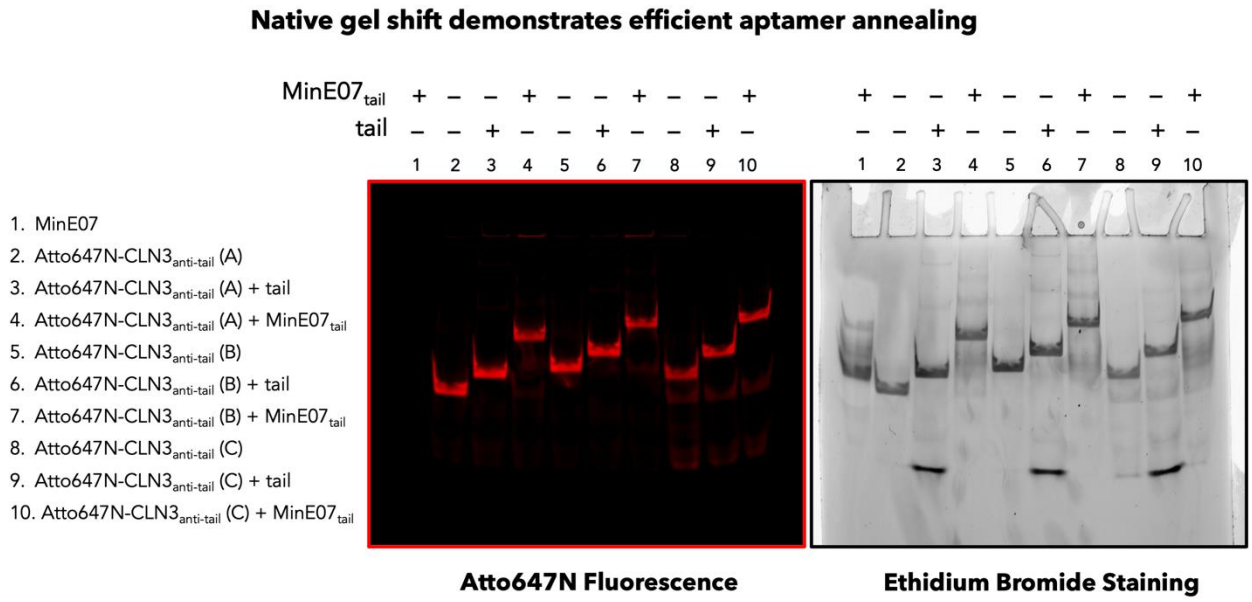

Figure S8. Electrophoretic mobility shift assay (EMSA) of engineered EGFR/c-Met bsApt. Effective formation of bsApt complexes was determined by EMSA. A molar ratio of 1:2 (antitail:tail) was used as follows: 20 pmol of Atto647N-CLN3$_t$ (A,B,C) were hybridized with 40 pmol of either MinE07$_{tail}$ or tail. Native 8% polyacrylamide gels (1x TBE) were first imaged to detect fluorescence of Atto647N-CLN3$_{anti\text{-}tail}$ and then ethidium bromide stained to visualize all oligonucleotide species. Interestingly, although MinE07 is a highly structured RNA oligonucleotide, its annealing efficiency with CLN3 was comparable with that of the shorter and less structured tail sequence (indeed >90% of Atto647N-CLN3anti-tail was effectively annealed with MinE07tail or tail). All oligonucleotide sequences are listed in Table S4.

Figure S9

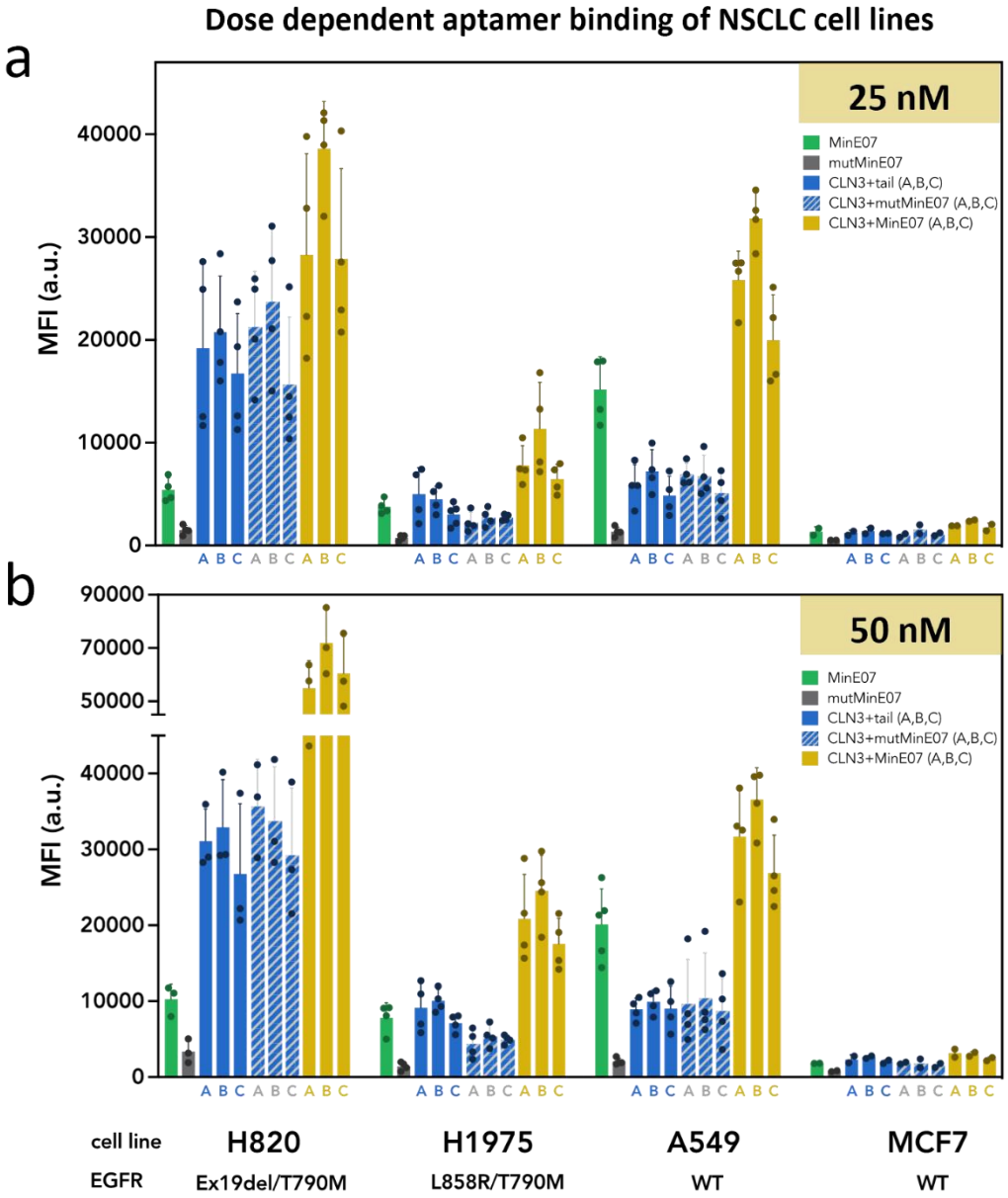

Figure S9. Monospecific and bispecific aptamer binding is dose dependent.
Cell lines harboring moderate to high levels (H820, H1975, A549) or very low levels (MCF7) of endogenous EGFR (WT or mutant) and c-Met (WT only) were incubated with (**a)** 25 nM or (**b**) 50 nM of Atto647N-labeled anti-EGFR (MinE07, green bars) or anti-c-Met (ABC variants of CLN3, blue bars) monospecific aptamer, EGFR/c-Met bispecific aptamer (yellow bars), or relevant control aptamers (mutMinE07, grey bars; mutMinE07 annealed to CLN3, blue/white bars) for 1 hr at 37°C and analyzed via flow cytometry. Labeling of both monospecific and bispecific aptamers to cell lines expressing moderate to high levels of endogenous EGFR and c-Met was dose dependent as absolute MFI values increased with dose, whereas only a minimal increase of background binding was observed with control aptamers. Plotted values (a, b) represent mean ± SD for n=2-5 independent experiments

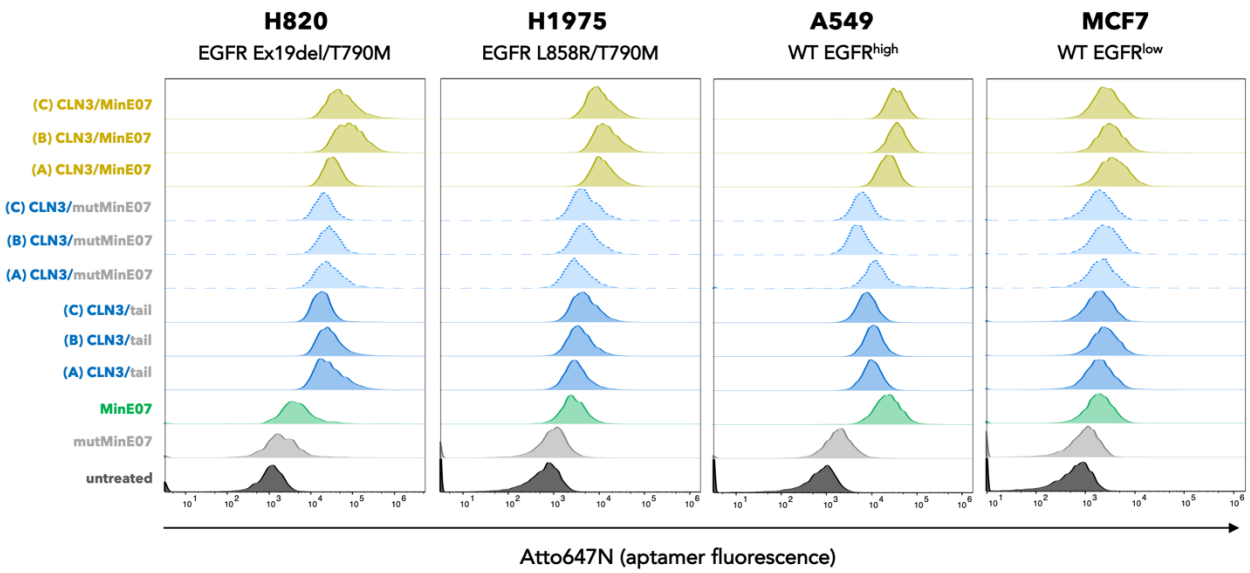

Figure S10. EGFR/c-Met bsApts (designs A, B, C) show superior cell labeling *in vitro* compared with monospecific aptamers and controls.
Representative flow cytometry histograms of cell labeling from Fig S10. Cells were incubated for 1 hr at 37°C with 50 nM Atto647N-labeled aptamer samples. Flow cytometry curves illustrate a clear shift in the cell staining for MinE07 (green) and CLN3 (blue) compared to control aptamer (mutMinE07, grey). The highest fluorescence shift could be seen when MinE07 was linked to CLN3 to yield bispecific aptamers.

Figure S11

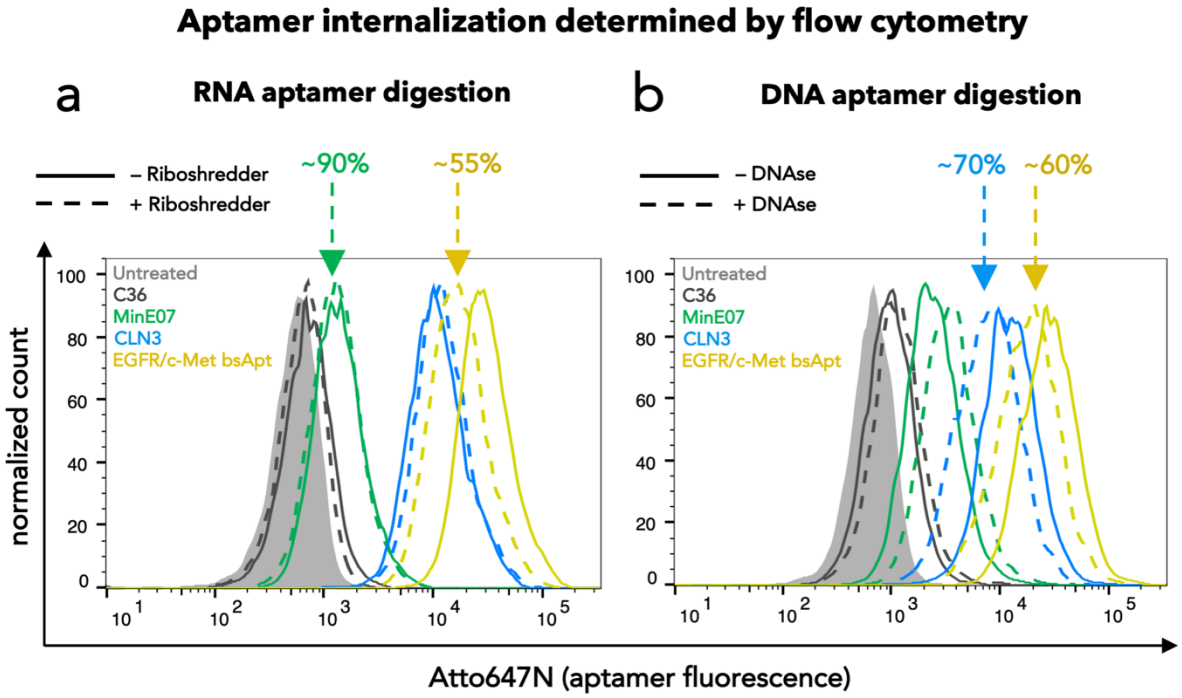

Figure S11. Anti-EGFR/c-Met bispecific aptamer is internalized similar to monospecific c-Met aptamer relative to total labeling.
(**a, b)** H1975 cells were incubated with 50 nM of Atto647N labeled anti-EGFR (MinE07, green histogram) or anti-c-Met (CLN3, blue histogram) monospecific aptamer, anti-EGFR/c-MET bispecific aptamer (yellow histogram), or relevant control aptamer (C36, black histogram) for 45 min at 37°C. Cells were then treated with either Riboshredder (dashed line, a), DNAse (dashed line b), or vehicle (solid line; a, b) for 30 min at 37°C to remove surface bound (non-internalized) aptamer. Cells were then analyzed via flow cytometry. Representative histograms from a single experiment are shown. n=1. Atto647N fluorescence is shown on the *x*-axis. Anti-EGFR (2'FY RNA) aptamer retained nearly 90% of its signal upon treatment with Riboshredder as opposed to the anti-EGFR/c-Met (2'FY RNA/DNA) bispecific aptamer which only retained ~55% of its signal. A similar level of signal was maintained for both the anti-c-Met (DNA) aptamer (~70%) and bispecific aptamer (~60%) when treated with DNAse. This likely suggests that the interactions of c-Met receptor and the anti-c-Met aptamer drive internalization properties of the bispecific aptamer.

Figure S12

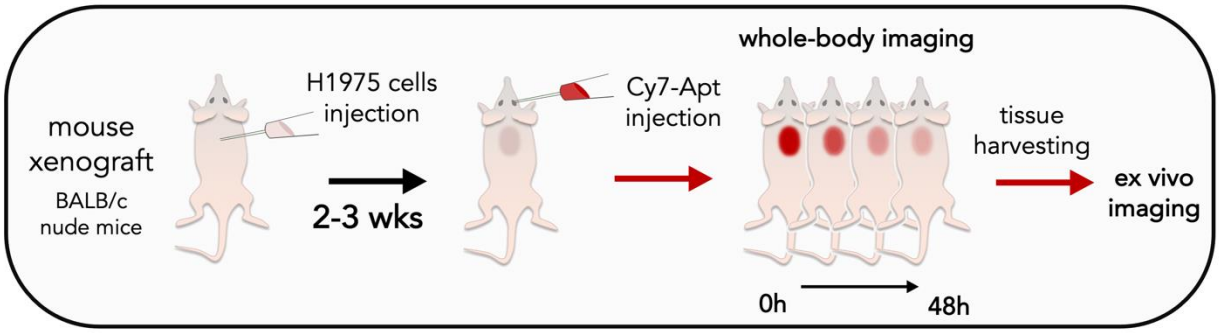

Figure S12. Schematic of *in vivo* biodistribution experiments.
Nude mice (6-8 weeks old) were subcutaneously implanted with approximately $5x10^6$ H1975 cells in 50% Matrigel in the right flank or shoulder and allowed to grow for 2-3 weeks until tumors reached ~50-150mm^2. When tumors reached appropriate size, mice were retro-orbitally injected with 50 pmol/g Cy7 labeled aptamer. Mice were anesthetized and imaged on the IVIS system at various timepoints over 48 hrs. At endpoint (48 hpi), mice were euthanized, vasculature was perfused with PBS, and major organs (liver, kidney, spleen, tumor, muscle) were harvested for *ex vivo* imaging and single cell analysis (*e.g.*, antigen expression, Fig S13).

Figure S13

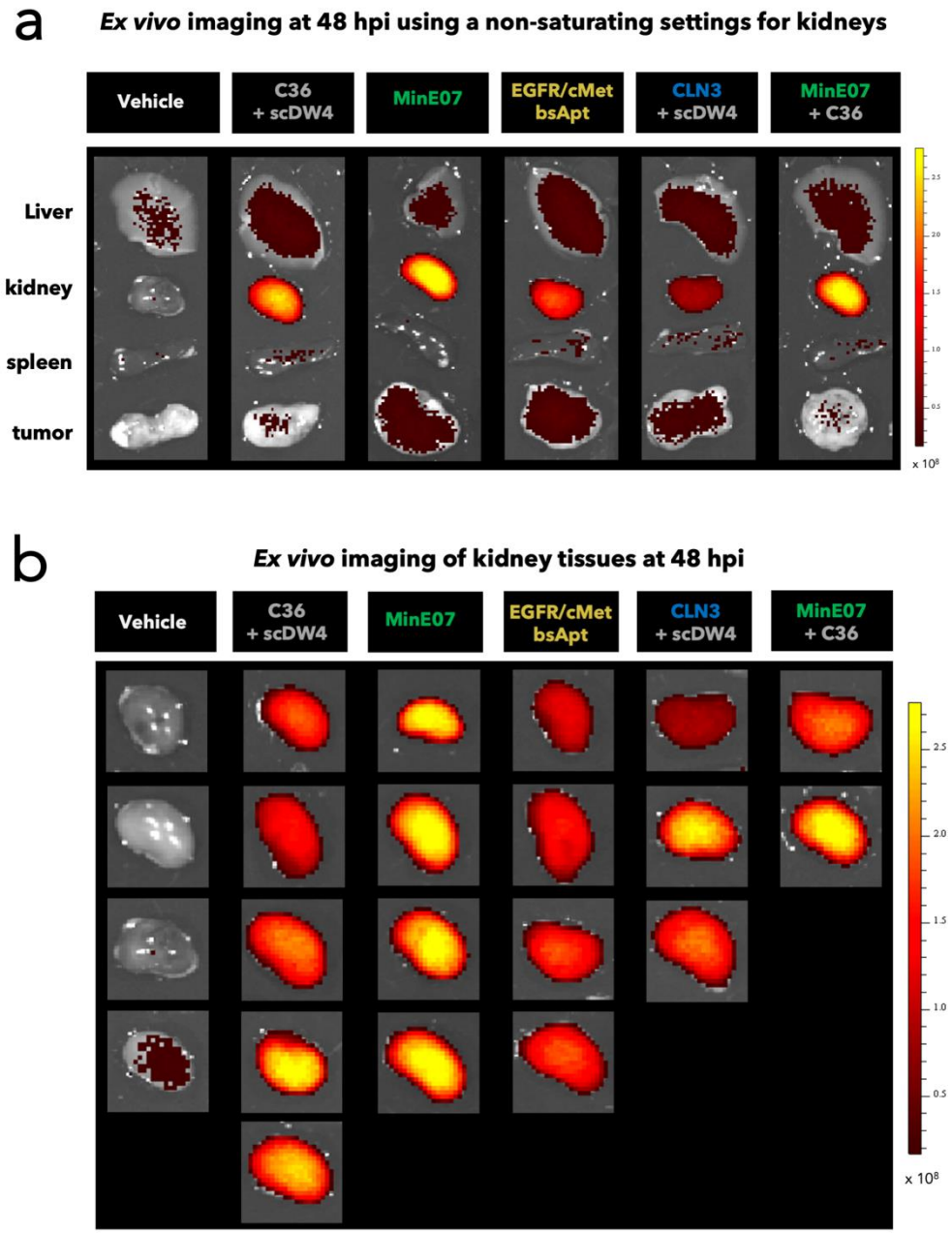

Figure S13. Endpoint biodistribution of monospecific and bispecific aptamers.
In both (a) and (b), a color scale was used that reduces overall fluorescence signal and avoids Cy7 saturation in kidney tissues. Color scale of radiant efficiency is Min= 1.69 x 10^7 Max= 2.78 x 10^8. (**a**) Representative *ex vivo* images of major organs (from top to bottom: liver, kidney, spleen, tumor) from one mouse per treatment is shown. Anti-EGFR monospecific aptamer (MinE07 annealed to anti-tail, green), anti-EGFR/c-Met bispecific aptamer (yellow), and anti-c-Met monospecific aptamer (CLN3 annealed to C36, blue/grey) localized to tumor relative to other aptamer constructs at 48 hpi. All Cy7-labeled aptamers localized to kidney and liver compared to vehicle (PBS) control. (**b**) *Ex vivo* images of all kidneys at 48 hpi. MinE07 annealed to anti-tail (green) had significantly higher radiant efficiency compared to the other aptamer samples. This can likely be attributed to glomerular filtration of the kidney (and subsequent cellular

uptake) in which smaller targeting aptamers (*e.g.*, aptamer annealed to anti-tail; ~28 kDa) are filtered quicker than larger aptamer constructs (*e.g.*, aptamer annealed to another targeting aptamer or control; ~50 kDa). n=2-5 mice (2 independent experiments).

Figure S14

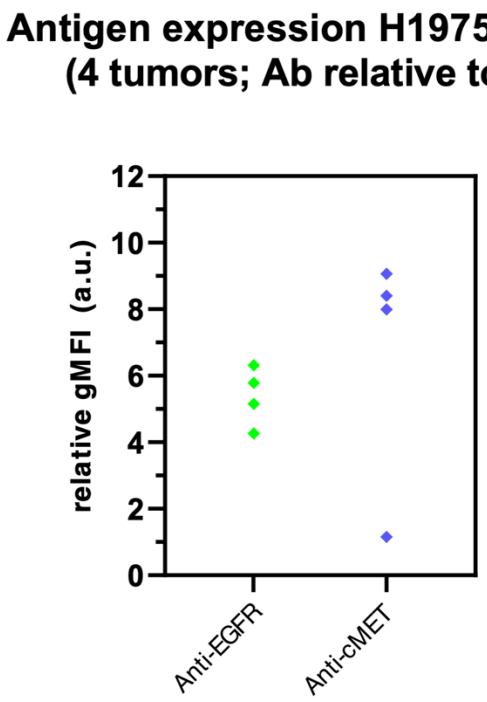

Figure S14. Anti-EGFR and anti-c-Met antibody labeling of tumor cells *ex vivo*.
When xenograft tumors reached the appropriate size, mice were euthanized, vasculature was perfused with PBS, and H1975-derived tumors were harvested and prepared into a single cell suspension. Cells were pre-blocked and then incubated with 4 µg/ml APC labeled anti-EGFR (clone AY13) and anti-c-Met (clone 271) antibodies, or 4 µg/ml APC labeled isotype control for 25 minutes and analyzed via flow cytometry. Relative geometric MFI (antibody/isotype) is reported on the *y*-axis. Analysis revealed that while EGFR and c-Met antigen expression is generally similar between mice, one mouse had significantly lower levels of c-Met expression (n = 4 mice).

Figure S15

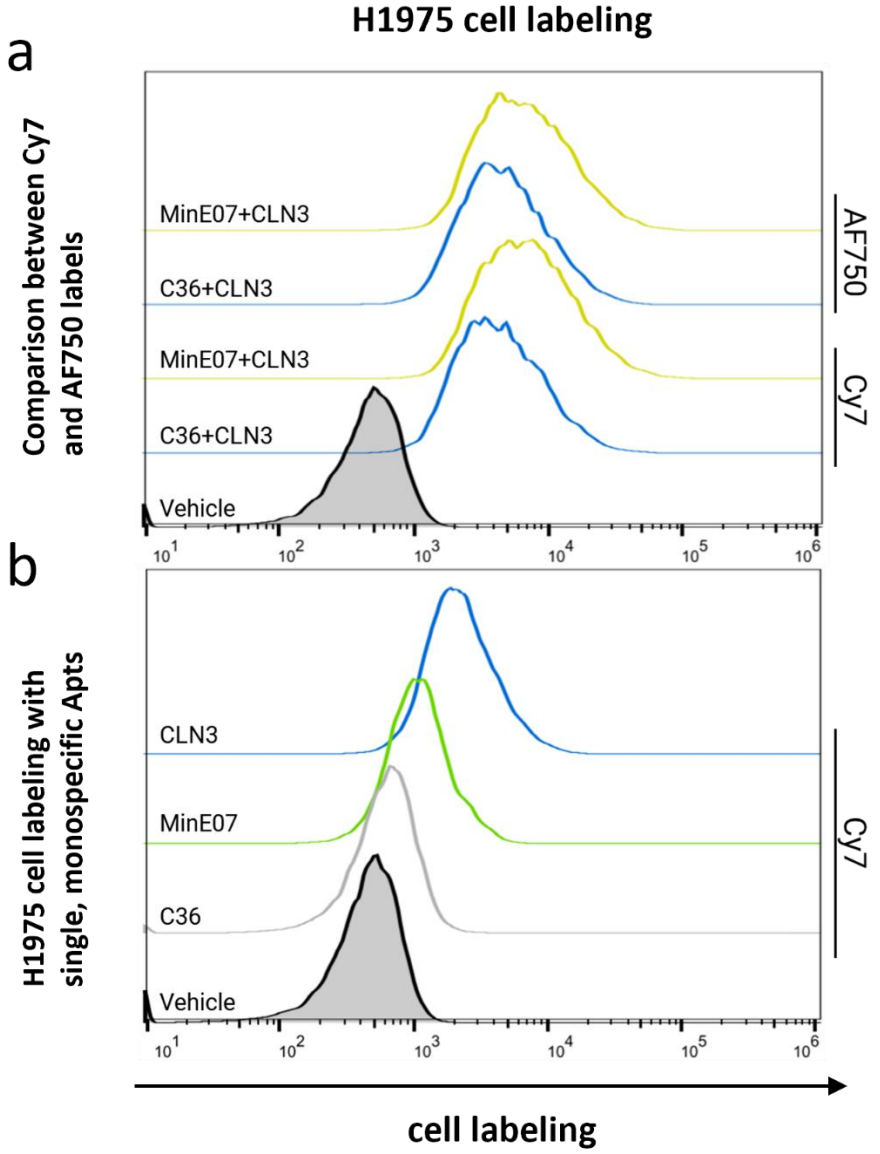

Figure S15. AF750 and Cy7 labeled bispecific aptamers stain NSCLC cells similarly *in vitro*.
(**a**) Labeling of H1975 cells upon 45 min incubation with 200 nM Cy7 or AF750 labeled CLN3 annealed to MinE07 (EGFR/c-Met bsApt, yellow), or negative control aptamer (C36+ CLN3, blue). (**b**) Labeling of H1975 cells upon 45 min incubation with 200 nM of Cy7 labeled MinE07 (green) or CLN3 (blue) monospecific aptamers, or negative control aptamer (C36, grey). Representative flow cytometry histograms from one of n = 2 independent experiments are shown. Cy7 or AF750 fluorescence is shown on the *x*-axis. The choice of fluorophore did not significantly affect bsApt labeling of H1975 cells *in vitro*.

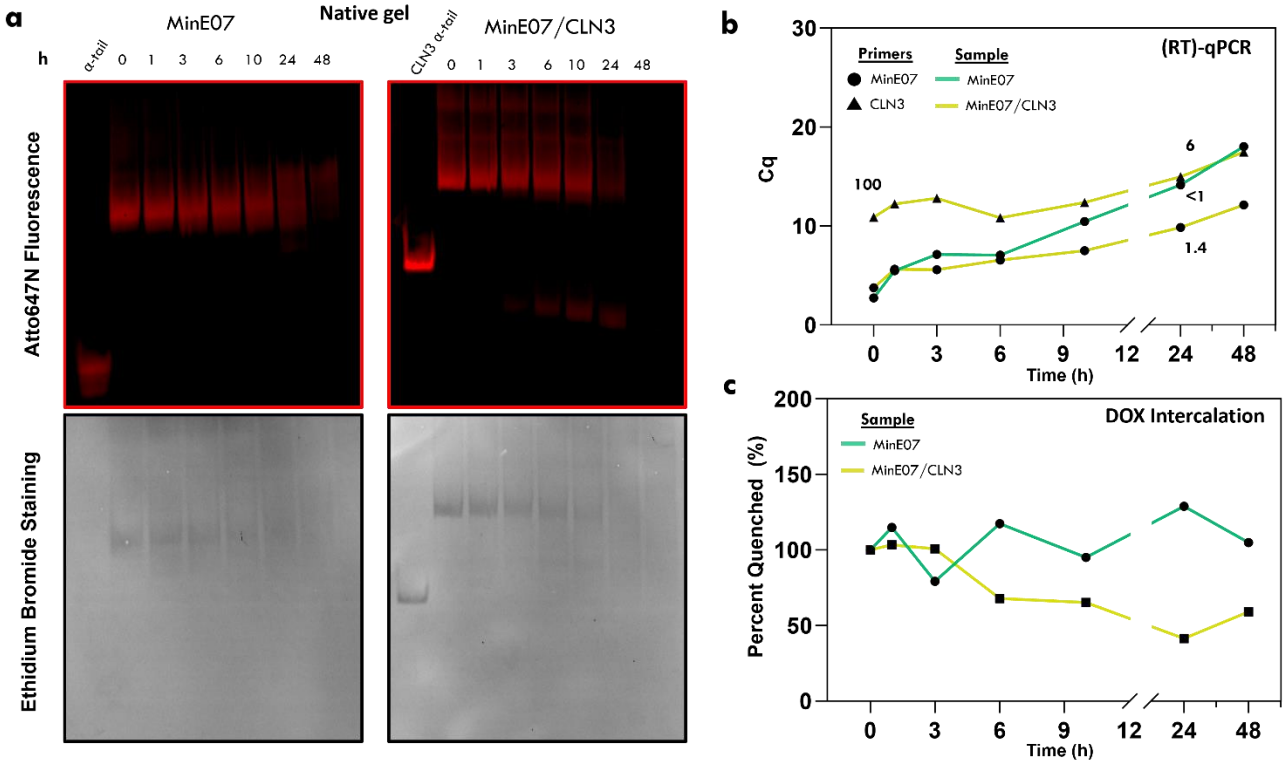

Figure S16. Aptamer stability in *in vivo* like conditions
To determine relative aptamer stability in *in vivo* like conditions, 500 nM Atto647N-labeled (**a**) or unlabeled (**b,c**) monospecific (MinE07) or bsApt (MinE07/CLN3) was incubated in 55% fetal bovine serum (FBS) in PBS for 0, 1, 3, 6, 10, 24, or 48 hours at 37°C in 5% CO_2. To degrade serum proteins prior to analysis, samples were treated with 1 mg/mL protK for 1 h at 37°C. (**a**) To determine the presence of full-length annealed aptamer, samples were run on native 8% polyacrylamide gels, stained with ethidium bromide, and imaged to detect Atto647N-labeled species (top) and all oligonucleotide species (bottom). (**b**) To determine the presence of mostly full-length aptamer, samples were diluted 1:100 in nuclease free water and subject to RT-qPCR (MinE07 primers; both aptamers) or qPCR (CLN3 primers; bsApt only). Percentages at 24 h represent the amount remaining relative to 0 h (100%) as calculated by the equation: $RE = 2^{-(Cq_t - Cq_{t0})}$. (**c**) To determine the presence of the hybridized tail/anti-tail, samples were mixed with 2 µM doxorubicin (DOX) and an emission scan was acquired (Ex 480 nm; Em 500-700 nm). Percent quenched is plotted where 100 percent represents the area under the curve (AUC) at 0 h (no serum) and 0 percent is the AUC of unannealed aptamer. Data shown represents one of n = 2 independent experiments. Full length aptamers were mostly degraded after 24 h in 55% serum. However, quenching of DOX, which is observed only when DOX intercalates with GC base pairs in the hybridized tail/anti-tail, was still present at ~50% (bsApt) and 100% (MinE07), suggesting that the hybridized tail/anti-tail was likely still present despite aptamer degradation.

Video S1. Single-molecule tracking of EGFR using MinE07 demonstrates formation of short-lived EGFR dimers on H1975 cells.

H1975 cells were incubated with 25 nM Atto647N-labeled MinE07 and single-molecule fluorescence imaging was performed. The video consists of a time-lapse sequence acquisition of diffraction-limited TIRF images and shows extended colocalization of two individual EGFRs labeled with MinE07 on the basal cell membrane. A clear increase of fluorescence intensity is detected upon colocalization. The lifetime of the colocalization event is ~1.9 sec (21 frames), suggesting that this is not due to random molecular collisions or stochastic colocalization (lifetime < 0.2 sec). TIRF microscopy was performed on a Leica SR GSD 3D microscope using a 160x objective lens (HC PL APO 160x /1.43, oil immersion), a 500-mW 642 nm laser (MPBC Inc., Montreal, Quebec, Canada), a 710/100 nm emission bandpass filter, and a EMCCD camera (iXon Ultra 897, Andor, UK). Time lapse sequences were recorded as previously described in Delcanale et al. (DOI: 10.1002/ange.202004764). Camera exposure time 50 ms; frame acquisition time (or total time per frame): 90 ms; laser intensity: 40% of maximum power. Total frames in video S1: 78. Video reproduction: 5 frames per sec. Scale bar 5 µm.

Table S1: Expression plasmids

Plasmid	Construct	Mutation*	Original Plamid
pBT002	pCMV EGFR_T2A_EGFP	ins (GSG) T2A	Addgene #32751
pBT003	pCMV EGFR (L858R)_T2A_EGFP	T to G (at 3297)	pBT002
pBT004	pCMV EGFR (delE746-A750)_T2A_EGFP	deletion 2959-2973	pBT002
pBT005	pCMV EGFR (delE747-A751insS)_T2A_EGFP	deletion 2964-2975	pBT002
pBT006	pCMV EGFR (L858R; T790M)_T2A_EGFP	C to T (at 3093)	pBT003
pBT007	pCMV EGFR (delE746-A750; T790M)_T2A_EGFP	C to T (at 3093)	pBT004
pMX016	pCMV EGFR (G465R)_T2A_EGFP	G to A (at 2117)	pBT002
pMX018	pCMV EGFR (S464L)_T2A_EGFP	C to T (at 2115)	pBT002
pMX019	pCMV EGFR (G465E)_T2A_EGFP	G to A (at 2118)	pBT002
pMX020	pCMV EGFR (S492R)_T2A_EGFP	C to A (at 2200)	pBT002

*Substitutions and deletions are reported as nucleotide location in the EGFR CDS

Table S2: Expression plasmid primer sets

Primer Set	Forward/ Reverse	Sequence (5' to 3')
1	F	ATGCGGGGACGTGGAGGAAAATCCCGGCCCAGTGAGCAAGGGCGAGGAG
	R	GTTAGAAGACTTCCCCTGCCCTCGCCGGAGCCTGCTCCAATAAATTCACTGC TTTG
2	F	GATTTTGGGCGGGCCAAACTG
	R	TGTGATCTTGACATGCTGC
3	F	AACATCTCCGAAAGCCAAC
	R	TTGATAGCGACGGGAATTTTAAC
4	F	CATCTCCGAAAGCCAACAAG
	R	ATTCCTTGATAGCGACGG
5	F	CAGCTCATCATGCAGCTCATGC
	R	CACGGTGGAGGTGAGGCA
6	F	GATAATTTCAAGAAACAAAAATTTGTG
	R	ACATCTCCATCACTTATC
7	F	TGTGATAATTTTAGGAAACAAAAATTTG
	R	TCTCCATCACTTATCTCC
8	F	GATAATTTCAGAAAACAAAAATTTGTGC
	R	ACATCTCCATCACTTATC
9	F	CAAAATTATAAGAAACAGAGGTGAAAAC
	R	GTTTTCTGACCGGAGGTC

Table S3: DNA templates and primers for the synthesis of 2'FY RNA aptamers

Aptamer	Template/Primer	Sequence (5' to 3')
MinE07	Template	GGACGGATTTAATCGCCGTAGAAAAGCATGTCAAAGCCGGAACC GTCCCGACGACGACGACGACGACGA
	F	GGATAATACGACTCACTATAGGACGGATTTAATCGC
	R	TCGTCGTCGTCGTCGTCGTCGGG
Mutant MinE07	Template	GGAGGTTAGACAGCAGGCGTAGAAAAGCATCATTTAGGACCAAC AACACGACGACGACGACGACGACGA
	F	GGATAATACGACTCACTATAGGAGGTTAGACAGCAG
	R	TCGTCGTCGTCGTCGTCGTCGTGTT
C36	Template	CTATAGGCGTAGTGATTATGAATCGTGTGCTAATACACGCCCGAC GACGACGACGACGACGACGA
	F	GGATAATACGACTCACTATAGGCGTAGTGATTATG
	R	TCGTCGTCGTCGTCGTCGTCGG

Table S4: 2'FY RNA aptamer and DNA aptamer sequences

	Sequence (5' to 3') (tail/anti-tail sequences are underlined)
MinE07$_{tail}$	GGACGGAUUUAAUCGCCGUAGAAAAGCAUGUCAAAGCCGGAACCGUCCCGACGACGACGACGACGACGA
mutMinE07$_{tail}$	GGAGGUUAGACAGCAGGCGUAGAAAAGCAUCAUUUAGGACCAACAACACGACGACGACGACGACGACGA
C36$_{tail}$	GGCGUAGUGAUUAUGAAUCGUGUGCUAAUACACGCCCGACGACGACGACGACGACGA
anti-tail	TCGTCGTCGTCGTCGTCGTCG
CLN3	ATCAGGCTGGATGGTAGCTCGGTCGGGGTGGGTGGGTTGGCAAGTCTGAT
CLN3$_{anti-tail}$ Design A	ATCAGGCTGGATGGTAGCTCGGTCGGGGTGGGTGGGTTGGCAAGTCTGATTATCGTCGTCGTCGTCGTCGTCG
CLN3$_{anti-tail}$ Design B	ATCAGGCTGGATGGTAGCTCGGTCGGGGTGGGTGGGTTGGCAAGTCTGATTATTTTTTTTTTTTTTCGTCGTCGTCGTCGTCGTCG
CLN3$_{anti-tail}$ Design C	ATCAGGCTGGATGGTAGCTCGGTCGGGGTGGGTGGGTTGGCAAGTCTGATTATCACGTACTCACGTGATCGTCGTCGTCGTCGTCGTCG
mutCLN3$_{anti-tail}$	ATCAGGCTGGTTGACAGCTCCTTCGATGTGGATGGGATGTCAAGTCTCATTATCGTCGTCGTCGTCGTCGTCGTCG
scDW4$_{anti-tail}$	GCCATTGCCATTGCCATTGCCATTGCCATTGCCATTGCCATTGCCATTGCCATTGTCGTCGTCGTCGTCGTCGTCG